

# A global residual-based stabilization for equal-order finite element approximations of incompressible flows

Douglas R. Q. Pacheco<sup>1,2</sup>  | Richard Schussnig<sup>2,3</sup> | Olaf Steinbach<sup>1,2</sup> | Thomas-Peter Fries<sup>2,3</sup> 

<sup>1</sup>Institute of Applied Mathematics, Graz University of Technology, Graz, Austria

<sup>2</sup>Graz Center of Computational Engineering, Graz University of Technology, Graz, Austria

<sup>3</sup>Institute of Structural Analysis, Graz University of Technology, Graz, Austria

## Correspondence

Douglas R. Q. Pacheco, Institute of Applied Mathematics, Graz University of Technology, Steyrergasse 30/III, Graz 8010, Austria.  
Email: pacheco@math.tugraz.at

## Funding information

Technische Universität Graz

## Abstract

Due to simplicity in implementation and data structure, elements with equal-order interpolation of velocity and pressure are very popular in finite-element-based flow simulations. Although such pairs are inf-sup unstable, various stabilization techniques exist to circumvent that and yield accurate approximations. The most popular one is the pressure-stabilized Petrov–Galerkin (PSPG) method, which consists of relaxing the incompressibility constraint with a weighted residual of the momentum equation. Yet, PSPG can perform poorly for low-order elements in diffusion-dominated flows, since first-order polynomial spaces are unable to approximate the second-order derivatives required for evaluating the viscous part of the stabilization term. Alternative techniques normally require additional projections or unconventional data structures. In this context, we present a novel technique that rewrites the second-order viscous term as a first-order boundary term, thereby allowing the complete computation of the residual even for lowest-order elements. Our method has a similar structure to standard residual-based formulations, but the stabilization term is computed globally instead of only in element interiors. This results in a scheme that does not relax incompressibility, thereby leading to improved approximations. The new method is simple to implement and accurate for a wide range of stabilization parameters, which is confirmed by various numerical examples.

## KEYWORDS

equal-order methods, incompressible flows, pressure boundary conditions, pressure Poisson equation, residual-based stabilization, stabilized finite element methods

## 1 | INTRODUCTION

In the early years of computational mechanics, there was considerable skepticism about whether the finite element method was a suitable technique for flow simulations. However, what was regarded as poor performance was rather the consequence of a numerical phenomenon commonly known as instability.<sup>1</sup> A classical example of an unstable formulation results from the use of linear interpolation for velocity and pressure in incompressible flows. The reason is that

This is an open access article under the terms of the Creative Commons Attribution-NonCommercial-NoDerivs License, which permits use and distribution in any medium, provided the original work is properly cited, the use is non-commercial and no modifications or adaptations are made.

© 2020 The Authors. *International Journal for Numerical Methods in Engineering* published by John Wiley & Sons Ltd.

equal-order pairs violate the Ladyzhenskaya–Babuška–Brezzi condition, which dictates a compatibility requirement for mixed finite element spaces.<sup>2</sup>

A major breakthrough came from Hood and Taylor,<sup>3</sup> who discovered that going one order higher in velocity allows stable, optimally convergent approximations. There is, however, great practical appeal in the use of equal-order interpolation for both flow quantities. The first so-called stabilized formulations allowing equal-order pairs were developed by Brezzi and Pitkäranta<sup>4</sup> and Hughes et al.<sup>5</sup> Both consist of perturbing the continuity equation to introduce a nonzero pressure–pressure block in the system, thereby breaking its saddle-point structure. The latter formulation<sup>5</sup>—often called pressure-stabilized Petrov–Galerkin (PSPG)<sup>6</sup>—has over the former<sup>4</sup> the advantage of being residual-based, that is, the added perturbation is proportional to the residual of the momentum equation. This means that the stabilization term is smaller in regions where the solution is accurate enough, quickly vanishing as the numerical solution converges to the exact one. Other residual-based stabilizations (RBS) similar to PSPG are also available.<sup>7–9</sup> Those are all efficient methods offering simple implementation, good accuracy and low computational cost, but they have something else in common: for linear elements, the velocity Laplacian in the residual cannot be approximated, which tends to result in loss of accuracy, especially for diffusion-dominated flows.<sup>10,11</sup>

One way to remedy the so-called spurious pressure boundary layers induced by the incomplete residual is to use interior penalty techniques<sup>10,12</sup> requiring edge/face-based data structures. The method proposed by Bochev and Gunzburger<sup>13</sup> avoids that by replacing the velocity Laplacian in the PSPG residual with a “discrete Laplacian” requiring only first-order derivatives. Yet, that demands the solution of an additional vector-valued global problem, which largely increases the size of the system to be solved. The stabilization by Jansen et al.<sup>11</sup> offers a reduced computational overhead by reconstructing the second-order derivatives on a local level. Other methods avoiding second-order derivatives are the so-called local projection stabilizations<sup>14,15</sup> which fit into the framework of variational multiscale methods. They demand considerably less computational effort than the original pressure gradient projection (PGP) method of Codina et al.,<sup>16,17</sup> which uses a global vector projection.

There exist other equal-order methods that are not based on residuals or gradient fluctuations, such as penalty,<sup>18</sup> artificial compressibility,<sup>19,20</sup> residual-free bubbles,<sup>21</sup> pressure–Poisson-based methods,<sup>22–24</sup> among others.<sup>25</sup> However, due to the simple structure and well-established robustness of residual-based methods, they are still the most popular choices in engineering applications. In this context, our present contribution introduces an RBS retaining the complete residual even for lowest-order elements, while also keeping a simple implementation (i.e., without the need for internal face/edge loops, macroelements or additional projections). The basic idea is to rewrite the Laplacian form in the weighted residual as a first-order boundary term. We achieve this by replacing the Navier–Stokes system by an equivalent boundary value problem (BVP). In our novel approach, the stabilization term is computed globally (instead of element-wise), whereas the continuity equation is handled in an element-weighted manner. With this, it is possible to construct a stabilized formulation that has a similar structure to other residual-based ones, but without relaxing incompressibility. We further show that our method is closely related to the family of pressure–Poisson-based formulations,<sup>22,23</sup> with the strong residual of the divergence-free constraint acting as an added penalty-like term. Numerical examples are provided in two and three dimensions, considering different types of elements and flow regimes. The results show a clear gain in accuracy with respect to the standard PSPG method, for a wider range of stabilization parameters. Also in examples with higher-order elements, our method shows a general increase in accuracy due to its improved conservation of mass.

It is important to note that the type of stabilization to which we herein refer is not to be confused with other residual-based techniques such as streamline upwind Petrov–Galerkin (SUPG),<sup>26</sup> grad–div,<sup>27,28</sup> or artificial diffusion.<sup>29</sup> Those methods aim to remedy other sources of instability/inaccuracy, and can be appropriately combined with the present one for specific flow problems and regimes. As a matter of fact, the SUPG technique employed for stabilizing convective effects also suffers from an incomplete residual evaluation in the lowest-order case. Nonetheless, in the flow regimes for which SUPG is actually important, the viscous terms typically have a minor contribution in the residual, so that the vanishing Laplacian is not a critical issue. For that reason, the present work focuses on—while not being limited to—the diffusion-dominated case. For an overview of finite element pressure stabilizations for incompressible flow problems, see References 30,31.

The rest of this article is organized as follows. In Section 2, we state the problem and briefly comment on usual issues. We start Section 3 by presenting the classical PSPG method and illustrating the matter of incomplete residuals for linear finite element spaces. Following that, our new stabilized formulation is presented in strong and weak forms. Section 4 deals with discretization and solution aspects, and Section 5 presents several numerical examples systematically comparing the performances of our new method and existing ones. We finally summarize our findings and draw relevant remarks.

## 2 | PROBLEM STATEMENT

As a model problem, we consider the homogeneous Dirichlet setting for the stationary incompressible Navier–Stokes system in a bounded Lipschitz domain  $\Omega \subset \mathbb{R}^d$ ,  $d = 2$  or  $3$ :

$$(\rho \nabla \mathbf{u}) \mathbf{u} - \mu \Delta \mathbf{u} + \nabla p = \rho \mathbf{g} \quad \text{in } \Omega, \quad (1)$$

$$\nabla \cdot \mathbf{u} = 0 \quad \text{in } \Omega, \quad (2)$$

$$\mathbf{u} = \mathbf{0} \quad \text{on } \Gamma := \partial\Omega, \quad (3)$$

where  $\mathbf{g}$  is a given volumetric force,  $\mathbf{u}$  is the flow velocity,  $p$  is the pressure, and  $\rho$  and  $\mu$  are the fluid's density and dynamic viscosity, respectively. In the pure Dirichlet case we apply the usual pressure scaling  $\int_{\Omega} p \, d\Omega = 0$ . The standard variational formulation for this problem is: Given  $\mathbf{g} \in X'$ , find  $(\mathbf{u}, p) \in X \times Y$  such that for all  $(\mathbf{w}, q) \in X \times Y$

$$\langle \mathbf{w}, (\rho \nabla \mathbf{u}) \mathbf{u} \rangle + \langle \nabla \mathbf{w}, \mu \nabla \mathbf{u} \rangle - \langle \nabla \cdot \mathbf{w}, p \rangle = \langle \mathbf{w}, \rho \mathbf{g} \rangle, \quad (4)$$

$$\langle q, \nabla \cdot \mathbf{u} \rangle = 0, \quad (5)$$

in which  $X = [H_0^1(\Omega)]^d$ ,  $X'$  is the dual space of  $X$ , and  $Y = L_0^2(\Omega) := \{q \in L^2(\Omega) : \int_{\Omega} q \, d\Omega = 0\}$ . Let  $X_h \subset X$  and  $Y_h \subset Y$  be discrete velocity and pressure spaces. The Bubnov–Galerkin finite element formulation reads: Given  $\mathbf{g} \in X'$ , find  $(\mathbf{u}_h, p_h) \in X_h \times Y_h$  such that for all  $(\mathbf{w}_h, q_h) \in X_h \times Y_h$

$$\langle \mathbf{w}_h, (\rho \nabla \mathbf{u}_h) \mathbf{u}_h \rangle + \langle \nabla \mathbf{w}_h, \mu \nabla \mathbf{u}_h \rangle - \langle \nabla \cdot \mathbf{w}_h, p_h \rangle = \langle \mathbf{w}_h, \rho \mathbf{g} \rangle, \quad (6)$$

$$\langle q_h, \nabla \cdot \mathbf{u}_h \rangle = 0. \quad (7)$$

The unique solvability in the infinite-dimensional case is not sufficient to guarantee that the discrete problem is also uniquely solvable, as  $X_h$  and  $Y_h$  must also be chosen carefully. In fact, for the simplest case where equal-order elements are used for velocity and pressure, the resulting system is in general *not* uniquely solvable (in other words, not invertible).<sup>1</sup> One way out is to use quadratic interpolation for velocity while keeping the pressure linear, which is the case of the well-known Taylor–Hood elements. Alternatively, it is possible to use equal-order pairs if the variational formulation is appropriately modified so as to break its saddle-point structure. Those are the so-called stabilized formulations, which are the focus here.

## 3 | STABILIZED FINITE ELEMENT FORMULATIONS

### 3.1 | The PSPG method

The PSPG method devised by Hughes et al.<sup>5</sup> is probably the most popular stabilization approach for incompressible flow simulations. It consists of keeping the momentum equation (6) as it is, while relaxing the incompressibility constraint (7) with an element-weighted residual of Equation (6):

$$\langle q_h, \nabla \cdot \mathbf{u}_h \rangle + \sum_{e=1}^{N_e} \langle \delta_e \nabla q_h, \nabla p_h - \mu \Delta \mathbf{u}_h + (\rho \nabla \mathbf{u}_h) \mathbf{u}_h - \rho \mathbf{g} \rangle_{\Omega_e} = 0, \quad (8)$$

where  $N_e$  is the number of elements  $\Omega_e$  and  $\delta_e$  is a positive parameter dependent on the element size  $h_e$ . In stationary Stokes flows or diffusion-dominated Navier–Stokes flows, for  $\delta_e = \alpha h_e^2 / \mu$  and sufficiently large  $\alpha$  the system formed by Equations (6) and (8) is stable for equal-order pairs.<sup>1,6</sup> Although diffusive regimes are in focus here, for completeness we present the approach commonly used in the general setting<sup>32</sup>:

$$\delta_e \sim \mathcal{O}(h_e^2 / \mu + h_e / |\mathbf{u}_h|), \quad (9)$$

where  $|\mathbf{u}_h|$  denotes the Euclidian norm of  $\mathbf{u}_h$ . The appropriate weights given to the different powers of  $h_e$  in Equation (9) depend on the problem and on the polynomial degree of the finite element spaces.<sup>1</sup>

The PSPG method is an efficient tool for incompressible flow simulations, offering computational simplicity and low cost. Nevertheless, it presents a drawback when lowest-order interpolations are used. For first-order triangular and rectangular elements (and their three-dimensional (3D) equivalents), the velocity Laplacian in the residual vanishes and Equation (8) reduces to

$$\langle q_h, \nabla \cdot \mathbf{u}_h \rangle + \sum_{e=1}^{N_e} \langle \delta_e \nabla q_h, \nabla p_h + (\rho \nabla \mathbf{u}_h) \mathbf{u}_h - \rho \mathbf{g} \rangle_{\Omega_e} = 0, \quad (10)$$

that is, the computation of the residual is incomplete, regardless of how fine the mesh is. Although this does not damage either the stability of the method or its global asymptotic convergence per se, it induces unphysical pressure boundary conditions (BCs)<sup>6</sup> and can lead to considerable loss of accuracy, often resulting in poor approximations.<sup>10,11</sup> In this context, devising a reformulation of the PSPG method retaining the viscous contribution in the residual for elements of any order is a relevant task.

*Remark 1.* In first-order nonsimplicial meshes, the velocity Laplacian will only be exactly zero in elements which are parallelograms (or parallelepipeds, in 3D).<sup>15</sup> However, even those elements where the Laplacian does not vanish completely have no approximation power for the viscous term, which can lead to inaccuracy.<sup>11</sup>

### 3.2 | A new pressure-Poisson-based stabilization

The first idea is to try relaxing the divergence-free constraint with a different form of the momentum equation, namely,

$$(\rho \nabla \mathbf{u}) \mathbf{u} + \mu \nabla \times (\nabla \times \mathbf{u}) + \nabla p = \rho \mathbf{g}, \quad (11)$$

which is equivalent to the standard Laplacian form.<sup>33,34</sup> This stems from the identity

$$\Delta \mathbf{u} \equiv \nabla (\nabla \cdot \mathbf{u}) - \nabla \times (\nabla \times \mathbf{u}) = -\nabla \times (\nabla \times \mathbf{u}).$$

Furthermore,

$$\nabla q \cdot [-\nabla \times (\nabla \times \mathbf{u})] \equiv \nabla \cdot [\nabla q \times (\nabla \times \mathbf{u})] - (\nabla \times \nabla q) \cdot (\nabla \times \mathbf{u}) = \nabla \cdot [\nabla q \times (\nabla \times \mathbf{u})],$$

since  $\nabla \times \nabla q \equiv \mathbf{0}$ . This allows us to write

$$\langle \nabla q, \mu \nabla \times \nabla \times \mathbf{u} \rangle_{\Omega_e} = - \int_{\Omega_e} \nabla \cdot [\nabla q \times (\mu \nabla \times \mathbf{u})] d\Omega = - \int_{\Gamma_e} \mathbf{n} \cdot [\nabla q \times (\mu \nabla \times \mathbf{u})] d\Gamma = \langle \nabla q \times \mathbf{n}, \mu \nabla \times \mathbf{u} \rangle_{\Gamma_e}, \quad (12)$$

where  $\Gamma_e := \partial\Omega_e$  and  $\mathbf{n}$  is the outward unit normal vector on  $\Gamma_e$ . We thus seem to have rewritten the second-order term as a computable first-order boundary term. Yet, as we will show next, this reformulation, as it is, does not offer an improvement with respect to PSPG. Let us assume simplicial elements with linear shape functions. If that is the case, all derivatives appearing in the formulation are piecewise constant, so that

$$\langle \nabla q_h \times \mathbf{n}, \mu \nabla \times \mathbf{u}_h \rangle_{\Gamma_e} = [\nabla q_h \times (\mu \nabla \times \mathbf{u}_h)] \cdot \int_{\Gamma_e} \mathbf{n} d\Gamma = 0,$$

since  $\int_S \mathbf{n} dS = \mathbf{0}$  for any closed region  $S$ . Hence, the modified viscous term vanishes again for linear elements, recovering the PSPG formulation. Nonetheless, we show next that a similar rewriting of the viscous term can be used globally (rather than element-wise) in order to overcome the incomplete residual.

Let us initially assume a uniform mesh, or at least a global definition of the mesh size in the stabilization parameter, so that  $\delta_e = \delta$  for all elements. Let us also assume continuous finite element trial and test spaces. Now, if we restrict the face integrals in Equation (12) only to the faces belonging to  $\partial\Omega$ , we get the equation

$$\delta^{-1} \langle q_h, \nabla \cdot \mathbf{u}_h \rangle + \langle \nabla q_h, \nabla p_h + (\rho \nabla \mathbf{u}_h) \mathbf{u}_h - \rho \mathbf{g} \rangle + \langle \nabla q_h \times \mathbf{n}, \mu \nabla \times \mathbf{u}_h \rangle_\Gamma = 0. \tag{13}$$

Now the face integral no longer vanishes, since the integrand is not constant over the whole boundary. The remaining question is how to treat local variations of the element size. As a matter of fact, we can generalize Equation (13) by changing  $\delta^{-1}$  back to  $\delta_e^{-1}$  in the divergence term:

$$\langle \nabla q_h, \nabla p_h + (\rho \nabla \mathbf{u}_h) \mathbf{u}_h - \rho \mathbf{g} \rangle + \langle \nabla q_h \times \mathbf{n}, \mu \nabla \times \mathbf{u}_h \rangle_\Gamma + \sum_{e=1}^{N_e} \langle \delta_e^{-1} q_h, \nabla \cdot \mathbf{u}_h \rangle_{\Omega_e} = 0. \tag{14}$$

So, in this modified version of PSPG, the roles of the stabilization term and the divergence form are somewhat inverted: the former is computed globally, while the latter is computed element-wise. We shall later comment on the implications of having a mesh-dependent factor on the divergence term.

A more formal way to derive our method starts from a modified BVP, as in many well-known stabilization techniques.<sup>4,8,23</sup> We propose the following BVP to replace the Navier–Stokes system (1)–(3):

$$(\rho \nabla \mathbf{u}) \mathbf{u} - \mu \Delta \mathbf{u} + \nabla p = \rho \mathbf{g} \quad \text{in } \Omega, \tag{15}$$

$$\Delta p = \nabla \cdot [\rho \mathbf{g} - (\rho \nabla \mathbf{u}) \mathbf{u}] + \gamma \nabla \cdot \mathbf{u} \quad \text{in } \Omega, \tag{16}$$

$$\frac{\partial p}{\partial n} = \mathbf{n} \cdot [\rho \mathbf{g} - (\rho \nabla \mathbf{u}) \mathbf{u} - \mu \nabla \times (\nabla \times \mathbf{u})] \quad \text{on } \Gamma, \tag{17}$$

$$\mathbf{u} = \mathbf{0} \quad \text{on } \Gamma, \tag{18}$$

where  $\gamma$  is some given positive function. We wish to show that, for sufficiently regular  $p$ ,  $\mathbf{u}$  and  $\mathbf{g}$ , this system is equivalent to the original Navier–Stokes problem.

**Lemma 1.** For  $p \in H^1(\Omega) \cap L_0^2(\Omega)$ ,  $\mathbf{u} \in [H^2(\Omega)]^d$ ,  $\mathbf{g} \in [L^2(\Omega)]^d$  and  $\gamma > 0$ , systems (15)–(18) and (1)–(3) are equivalent.

*Proof.* Under the regularity requirements stated above, Heywood and Rannacher<sup>35</sup> proved that the standard Navier–Stokes system implies Equation (16) with  $\gamma = 0$ , and the case  $\gamma \neq 0$  follows immediately. Therefore, what remains is to show the other direction. The first step is to apply the divergence operator to both sides of Equation (15), yielding

$$\Delta p = \nabla \cdot [\rho \mathbf{g} - (\rho \nabla \mathbf{u}) \mathbf{u} + \mu \Delta \mathbf{u}] = \nabla \cdot [\rho \mathbf{g} - (\rho \nabla \mathbf{u}) \mathbf{u}] + \mu \Delta (\nabla \cdot \mathbf{u}), \tag{19}$$

which is the so-called pressure Poisson equation (PPE). Subtracting Equation (19) from Equation (16) leads to a diffusion-reaction equation in the variable  $\phi := \nabla \cdot \mathbf{u}$ :

$$\Delta \phi - \frac{\gamma}{\mu} \phi = 0 \quad \text{in } \Omega. \tag{20}$$

The boundary condition (BC) for this equation can be obtained by dotting both sides of Equation (15) with  $\mathbf{n}$  and subtracting the result from Equation (17), which gives

$$0 = \mathbf{n} \cdot [\Delta \mathbf{u} + (\nabla \times \nabla \times \mathbf{u})] = \mathbf{n} \cdot [\nabla (\nabla \cdot \mathbf{u})] = \frac{\partial \phi}{\partial n}. \tag{21}$$

We have then a homogeneous diffusion-reaction equation with zero Neumann BC. For  $\gamma/\mu > 0$ , the result is the trivial solution  $\phi \equiv 0$ , that is,  $\nabla \cdot \mathbf{u} = 0$  in  $\Omega$ , as wanted. ■

Now, we can derive a variational formulation for the equivalent system. We begin by multiplying Equation (16) by a test function  $q \in H^1(\Omega)$  and integrating over  $\Omega$ :

$$\langle \gamma q, \nabla \cdot \mathbf{u} \rangle - \langle q, \Delta p - \nabla \cdot [\rho \mathbf{g} - (\rho \nabla \mathbf{u}) \mathbf{u}] \rangle = 0. \tag{22}$$

Applying integration by parts to the second term gives us

$$\langle \gamma q, \nabla \cdot \mathbf{u} \rangle + \langle \nabla q, \nabla p + (\rho \nabla \mathbf{u}) \mathbf{u} - \rho \mathbf{g} \rangle - \left\langle q, \frac{\partial p}{\partial n} + \mathbf{n} \cdot [(\rho \nabla \mathbf{u}) \mathbf{u} - \rho \mathbf{g}] \right\rangle_{\Gamma} = 0. \quad (23)$$

Now, we substitute the Neumann BC (17) to get

$$\langle \gamma q, \nabla \cdot \mathbf{u} \rangle + \langle \nabla q, \nabla p + (\rho \nabla \mathbf{u}) \mathbf{u} - \rho \mathbf{g} \rangle + \mu \langle q, \mathbf{n} \cdot [\nabla \times (\nabla \times \mathbf{u})] \rangle_{\Gamma} = 0. \quad (24)$$

The divergence theorem can be used to write

$$\langle q, \mathbf{n} \cdot [\nabla \times (\nabla \times \mathbf{u})] \rangle_{\Gamma} = \int_{\Omega} \nabla \cdot [q \nabla \times (\nabla \times \mathbf{u})] \, d\Omega,$$

but

$$\nabla \cdot [q \nabla \times (\nabla \times \mathbf{u})] = \nabla q \cdot [\nabla \times (\nabla \times \mathbf{u})] + q \nabla \cdot [\nabla \times (\nabla \times \mathbf{u})] = \nabla q \cdot [\nabla \times (\nabla \times \mathbf{u})].$$

Moreover,

$$\langle \nabla q, \nabla \times (\nabla \times \mathbf{u}) \rangle \equiv \int_{\Omega} \nabla \cdot [(\nabla \times \mathbf{u}) \times \nabla q] + (\nabla \times \nabla q) \cdot (\nabla \times \mathbf{u}) \, d\Omega = \int_{\Omega} \nabla \cdot [(\nabla \times \mathbf{u}) \times \nabla q] \, d\Omega = \langle \nabla q \times \mathbf{n}, \nabla \times \mathbf{u} \rangle_{\Gamma}, \quad (25)$$

so that the weak form of our stabilized equation becomes

$$\langle \gamma q, \nabla \cdot \mathbf{u} \rangle + \langle \nabla q, \nabla p \rangle + \langle \nabla q, (\rho \nabla \mathbf{u}) \mathbf{u} \rangle + \langle \nabla q \times \mathbf{n}, \mu \nabla \times \mathbf{u} \rangle_{\Gamma} = \langle \nabla q, \rho \mathbf{g} \rangle. \quad (26)$$

*Remark 2.* In showing the equivalence between the PPE-based system and the original Navier–Stokes BVP (Lemma 1), we have required  $p \in H^1(\Omega)$  and  $\mathbf{u} \in [H^2(\Omega)]^d$ . A slightly less restrictive proof considering the weak problem was presented by Sani et al.<sup>36</sup> for the “pure PPE” ( $\gamma = 0$ ) and can be extended to the present case. Although their proof requires  $\nabla p - \mu \Delta \mathbf{u} \in [L^2(\Omega)]^d$ , which is still more restrictive than standard weak formulations, there is substantial numerical evidence that such PPE-based methods provide accurate approximations even for problems with singularities.<sup>23,24,37–42</sup>

### 3.2.1 | Regularity assumptions and their finite element realization

The fact that the stabilization term is computed globally in our PPE-based formulation leads to different regularity requirements than in the standard PSPG formulation. Notice that, in deriving Equation (25), we require  $\nabla \times \nabla q \in [L^2(\Omega)]^d$ , that is,  $\nabla q \in H(\text{curl}, \Omega)$ . Fortunately, this condition is fulfilled by  $q \in H^1(\Omega)$ ,<sup>23</sup> which can be shown through a Helmholtz decomposition of  $H(\text{curl}, \Omega)$  (cf. 43, theorem 29). Furthermore, due to the boundary term, we have the requirement  $\mathbf{n} \times \nabla q \in [L^2(\Gamma)]^d$ . Regarding the pressure trial space  $Y$ , we need  $p \in H^1(\Omega)$  to ensure boundedness of the bilinear form  $\langle \nabla q, \nabla p \rangle$ .

For the velocity test space  $X$  we can take simply  $[H_0^1(\Omega)]^d$ . Due to the boundary term, for the velocity trial space  $\tilde{X}$  we get the additional requirement  $(\nabla \times \mathbf{u})|_{\Gamma} \in [L^2(\Gamma)]^d$ . Another interesting regularity aspect comes from the nonlinear term in the PPE. Notice that boundedness of the form  $\langle \nabla q, (\rho \nabla \mathbf{u}) \mathbf{u} \rangle$  is *not* guaranteed by having simply  $\mathbf{u} \in [H^1(\Omega)]^d$ . In fact, we can derive sufficient conditions by using the Sobolev embedding<sup>6</sup>  $[H^1(\Omega)]^d \subset [L^m(\Omega)]^d$ , with  $m \in [1, \infty)$  for  $d = 2$  and  $m \in [1, 6]$  for  $d = 3$ . Therefore, due to Hölder’s inequality, the condition  $[(\nabla \mathbf{u}) \mathbf{u}] \in [L^2(\Omega)]^d$  is trivially satisfied by  $\mathbf{u} \in [H^1(\Omega)]^d$  in the two-dimensional (2D) case, whereas for  $d = 3$  we need  $\nabla \mathbf{u} \in [L^3(\Omega)]^{d \times d}$ .

At last, we remark that the usual condition  $\mathbf{g} \in [H^{-1}(\Omega)]^d$  is not sufficient to bound the right-hand side of Equation (26). We then take  $\mathbf{g} \in [L^2(\Omega)]^d$ . Finally, we can state our variational formulation as: Given  $\mathbf{g} \in [L^2(\Omega)]^d$ , find  $(\mathbf{u}, p) \in \tilde{X} \times Y$  such that for all  $(\mathbf{w}, q) \in X \times \tilde{Y}$

$$\langle \mathbf{w}, (\rho \nabla \mathbf{u}) \mathbf{u} \rangle + \langle \nabla \mathbf{w}, \mu \nabla \mathbf{u} \rangle - \langle \nabla \cdot \mathbf{w}, p \rangle = \langle \mathbf{w}, \rho \mathbf{g} \rangle, \quad (27)$$

$$\langle \gamma q, \nabla \cdot \mathbf{u} \rangle + \langle \nabla q, \nabla p \rangle + \langle \nabla q, (\rho \nabla \mathbf{u}) \mathbf{u} \rangle + \langle \nabla q \times \mathbf{n}, \mu \nabla \times \mathbf{u} \rangle_{\Gamma} = \langle \nabla q, \rho \mathbf{g} \rangle, \quad (28)$$

with  $X = [H_0^1(\Omega)]^d$ ,  $Y = H^1(\Omega) \cap L_0^2(\Omega)$ ,  $\tilde{Y} = \left\{ q \in Y : \mathbf{n} \times \nabla q|_{\Gamma} \in [L^2(\Gamma)]^d \right\}$  and

$$\tilde{X} = \begin{cases} \left\{ \mathbf{w} \in X : (\nabla \times \mathbf{w})|_{\Gamma} \in [L^2(\Gamma)]^d \right\}, & \text{if } d = 2, \\ \left\{ \mathbf{w} \in X : (\nabla \times \mathbf{w})|_{\Gamma} \in [L^2(\Gamma)]^d \text{ and } \nabla \mathbf{w} \in [L^3(\Omega)]^{d \times d} \right\}, & \text{if } d = 3. \end{cases} \quad (29)$$

It is important to remark that, although these spaces may seem somewhat unusual on the continuous level, their regularity requirements are fulfilled by standard  $C^0$  Lagrangian finite element spaces.<sup>22</sup> This is due to the fact that the derivatives of continuous Lagrangian basis functions are piecewise polynomial and therefore integrable to any power, both in the domain and on the boundary.

### 3.2.2 | Discrete formulation and stabilization parameter

A last question to answer is how to formally define the function  $\gamma$  that acts as a weight for the divergence bilinear form. For conformity, it is sufficient to take  $\gamma \in L^3(\Omega)$ , that is, the usual piecewise constant stabilization parameters are allowed. Also notice that  $\gamma$  appears in the reaction term of Equation (20), so it must be positive in order to guarantee  $\nabla \cdot \mathbf{u} \equiv 0$ . In the discrete case,  $\gamma$  must be chosen appropriately if we desire optimal velocity convergence. For that, we compare our formulation to the modified PSPG form of Brezzi and Douglas Jr,<sup>8</sup> which is defined for quasi-uniform meshes. In that case, their relaxed continuity equation is written as

$$\langle q, \nabla \cdot \mathbf{u} \rangle + \frac{\alpha h^2}{\mu} \left[ \langle \nabla q, \nabla p \rangle + \langle \nabla q, (\rho \nabla \mathbf{u}) \mathbf{u} \rangle + \langle q \mathbf{n}, \mu \Delta \mathbf{u} \rangle_{\Gamma} - \langle \nabla q, \rho \mathbf{g} \rangle \right] = 0. \quad (30)$$

As in our method, they treat the viscous contribution as a boundary term—but with a second-order operator, which again reduces the method to standard PSPG if linear elements are used. Comparing our form (28) to theirs (30) (or any classical stabilized formulation fitting the present framework<sup>4,5,7-9,16</sup>) leads to a natural choice for  $\gamma$ , namely,  $\gamma = (\alpha h^2 / \mu)^{-1}$ , or  $\gamma_e = (\alpha h_e^2 / \mu)^{-1}$  for nonuniform meshes. Of course, since  $\gamma_e$  is basically the inverse of the PSPG parameter  $\delta_e$ , a different expression should be used for convection-dominated flows, as previously shown in Equation (9).

We are finally in position to state our finite element formulation. Considering a more general setting with Dirichlet data  $\mathbf{u}|_{\Gamma_D} = \mathbf{u}_D$  and natural data  $[(\mu \nabla \mathbf{u}) \mathbf{n} - p \mathbf{n}]|_{\Gamma_N} = \mathbf{t}_N$ , the discrete problem reads: Given  $\mathbf{g} \in [L^2(\Omega)]^d$ , find  $(\mathbf{u}_h, p_h) \in X_h \times Y_h$ , with  $\mathbf{u}_h|_{\Gamma_D} = \mathbf{u}_D$ , such that for all  $(\mathbf{w}_h, q_h) \in X_h \times Y_h$ , with  $\mathbf{w}_h|_{\Gamma_D} = \mathbf{0}$ ,

$$\begin{aligned} & \langle \mathbf{w}_h, (\rho \nabla \mathbf{u}_h) \mathbf{u}_h \rangle + \langle \nabla \mathbf{w}_h, \mu \nabla \mathbf{u}_h \rangle - \langle \nabla \cdot \mathbf{w}_h, p_h \rangle = \langle \mathbf{w}_h, \rho \mathbf{g} \rangle + \langle \mathbf{w}_h, \mathbf{t}_N \rangle_{\Gamma_N} \\ & \langle \nabla q_h, \nabla p_h + (\rho \nabla \mathbf{u}_h) \mathbf{u}_h \rangle + \langle \nabla q_h \times \mathbf{n}, \mu \nabla \times \mathbf{u}_h \rangle_{\Gamma} + \sum_{e=1}^{N_e} \langle \gamma_e q_h, \nabla \cdot \mathbf{u}_h \rangle_{\Omega_e} = \langle \nabla q_h, \rho \mathbf{g} \rangle, \end{aligned} \quad (31)$$

with  $X_h$  and  $Y_h$  taken as  $C^0$  finite element spaces for conformity.

It is worth remarking that, if  $\gamma \rightarrow 0$ , that is,  $\alpha \rightarrow \infty$ , the pressure Poisson formulation by Johnston and Liu<sup>22</sup> is recovered. Their method replaces the continuity equation by the PPE completely, which leads to a stable but suboptimally convergent scheme when equal-order pairs are used.<sup>23,37</sup> Hence, our formulation can be given two quite distinct interpretations. On the one hand, it can be viewed as a modification of PSPG dealing with mesh size effects in the divergence term rather than in the stabilization term; on the other hand, one can also see our method as a PPE-based formulation<sup>23,24</sup> with an added term penalizing violations of the divergence-free constraint. An important consequence is that, differently from standard residual-based methods, ours does not relax incompressibility. In the standard formulations,  $\alpha \rightarrow \infty$  leads to the stabilizing term replacing completely the continuity equation, that is, the system no longer conserves mass (not even approximately). In our formulation,  $\alpha \rightarrow \infty$  means completely replacing the continuity equation by the PPE, which also enforces incompressibility, but in a lower-order way (see References 23,24,44 for excellent discussions on how different forms of the PPE can be used to enforce conservation of mass). We also remark that, even when using higher-order finite element spaces, our method does not require second-order derivatives of shape functions, which represents an advantage from the standpoint of implementation and data structure.

### 3.2.3 | Interpretation as a pressure-gradient-fluctuation method

Similarly to other stabilizations methods,<sup>15,16</sup> ours can also be given distinct interpretations. In his book, V. John<sup>6</sup> includes global<sup>16</sup> and local<sup>15</sup> pressure projection methods into the framework of stabilization techniques based on fluctuations of the pressure gradient. That started with Codina and Blasco,<sup>16</sup> who solved the issue of spurious pressure boundary layers (in the original method by Brezzi and Pitkäranta<sup>4</sup>) by replacing the pressure gradient in the stabilization term by the fluctuation  $\nabla p_h - \overline{\nabla p_h}$ , with  $\overline{\nabla p_h}$  denoting the  $L^2$  projection of  $\nabla p_h$  onto the (unconstrained) velocity space. For the Stokes system with homogenous Dirichlet BCs, their PGP method reads: Find  $(\mathbf{u}_h, p_h, \overline{\nabla p_h}) \in (X_h \cap H_0^1(\Omega))^d \times X_h \times X_h^d$ , such that for all  $(\mathbf{w}_h, q_h, \mathbf{v}_h) \in (X_h \cap H_0^1(\Omega))^d \times X_h \times X_h^d$

$$\begin{aligned} \langle \nabla \mathbf{w}_h, \mu \nabla \mathbf{u}_h \rangle - \langle \nabla \cdot \mathbf{w}_h, p_h \rangle &= \langle \mathbf{w}_h, \rho \mathbf{g} \rangle, \\ \langle q_h, \nabla \cdot \mathbf{u}_h \rangle + \sum_{e=1}^{N_e} \frac{\alpha h_e^2}{\mu} \langle \nabla q_h, \nabla p_h - \overline{\nabla p_h} \rangle_{\Omega_e} &= 0, \\ \langle \mathbf{v}_h, \overline{\nabla p_h} \rangle &= \langle \mathbf{v}_h, \nabla p_h \rangle, \end{aligned} \quad (32)$$

with  $X_h \subset H^1(\Omega)$ . A similar idea is used for local pressure projection methods,<sup>15</sup> but employing local fluctuation operators to avoid the computational overhead of solving a global problem for  $\overline{\nabla p_h}$ .

As it turns out, we can also write our new formulation as a fluctuation-based stabilization, but replacing  $\overline{\nabla p_h}$  by  $\nabla \tilde{p}_h$ , with  $\tilde{p}_h$  being the solution of the PPE.<sup>22</sup> The system would then be: Find  $(\mathbf{u}_h, p_h, \tilde{p}_h) \in (X_h \cap H_0^1(\Omega))^d \times Y_h \times Y_h$ , such that for all  $(\mathbf{w}_h, q_h, \tilde{q}_h) \in (X_h \cap H_0^1(\Omega))^d \times Y_h \times \tilde{Y}_h$

$$\langle \nabla \mathbf{w}_h, \mu \nabla \mathbf{u}_h \rangle - \langle \nabla \cdot \mathbf{w}_h, p_h \rangle = \langle \mathbf{w}_h, \rho \mathbf{g} \rangle, \quad (33)$$

$$\sum_{e=1}^{N_e} \frac{\mu}{\alpha h_e^2} \langle q_h, \nabla \cdot \mathbf{u}_h \rangle_{\Omega_e} + \langle \nabla q_h, \nabla p_h - \nabla \tilde{p}_h \rangle = 0, \quad (34)$$

$$\langle \nabla \tilde{q}_h, \nabla \tilde{p}_h \rangle = \langle \mathbf{n} \times \nabla \tilde{q}_h, \mu \nabla \times \mathbf{u}_h \rangle_{\Gamma} + \langle \nabla \tilde{q}_h, \rho \mathbf{g} \rangle, \quad (35)$$

with  $Y_h, X_h$ , and  $\tilde{Y}_h$  being continuous finite element spaces. If we choose  $\tilde{Y}_h = Y_h$  for the discretization, it is easy to verify that the elimination of  $\tilde{p}_h$  leads straight to our original stabilized system (31). The underlying idea in the above formulation is to penalize fluctuations of the original pressure with respect to the stable pressure coming from the PPE. The key ingredient for efficiency here is accounting for mesh size variations in the divergence term and not in the stabilization term. Otherwise, it would not be possible to directly substitute the term  $\langle \nabla \tilde{q}_h, \nabla \tilde{p}_h \rangle$  from Equation (35) into Equation (34) without first solving for  $\tilde{p}_h$ .

### 3.2.4 | Stability for nonuniform meshes

One of the main distinct aspects of our stabilized method is the presence of the stabilization parameter in the divergence term. This means that, even if we were to drop the nonlinearity and the boundary term, the resulting formulation would still be asymmetric, since the divergence term in the continuity equation is no longer adjoint to the pressure term in the momentum equation. Furthermore, the “weighted divergence” can complicate the stability analysis. In order to illustrate that, let us consider, for the Stokes problem, a scaled version of our variational formulation where the (stabilized) continuity equation is multiplied by  $\alpha h^2/\mu$ , with  $h$  being the maximum element size (note that this is a simple scaling and does not change the solution). Then, we can combine the momentum and continuity equations in one bilinear form:

$$A((\mathbf{u}_h, p_h), (\mathbf{w}_h, q_h)) = \langle \nabla \mathbf{w}_h, \mu \nabla \mathbf{u}_h \rangle - \langle \nabla \cdot \mathbf{w}_h, p_h \rangle + \frac{\alpha h^2}{\mu} [\langle \nabla q_h, \nabla p_h \rangle + \langle \nabla q_h \times \mathbf{n}, \mu \nabla \times \mathbf{u}_h \rangle_{\Gamma}] + \sum_e \frac{h^2}{h_e^2} \langle q_h, \nabla \cdot \mathbf{u}_h \rangle_{\Omega_e}. \quad (36)$$

When proving stability for residual-based formulations, the most common approach is to show coercitivity of  $A$  over a mesh-dependent norm to use the theorem of Lax–Milgram.<sup>5</sup> We have



$$A((\mathbf{u}_h, p_h), (\mathbf{u}_h, p_h)) = \langle \nabla \mathbf{u}_h, \mu \nabla \mathbf{u}_h \rangle + \frac{\alpha h^2}{\mu} [\langle \nabla p_h, \nabla p_h \rangle + \langle \nabla p_h \times \mathbf{n}, \mu \nabla \times \mathbf{u}_h \rangle_\Gamma] + \sum_e^{N_e} \left[ \left( \frac{h}{h_e} \right)^2 - 1 \right] \langle p_h, \nabla \cdot \mathbf{u}_h \rangle_{\Omega_e}. \quad (37)$$

For a uniform mesh, we have  $(h/h_e)^2 - 1 = 0$  for all elements, so the divergence term vanishes and we can apply standard techniques used in classical RBSs (provided that the boundary term is also appropriately estimated<sup>8</sup>). If we no longer have a uniform mesh but a globally quasi-uniform one, that is,

$$1 \leq \frac{h}{h_e} \leq C \text{ for all elements, with } C \geq 1, \quad (38)$$

using the Cauchy-Schwarz and Young's inequalities we can write

$$\langle p_h, \nabla \cdot \mathbf{u}_h \rangle_{\Omega_e} \geq -\|p_h\|_{L^2(\Omega_e)} \|\nabla \cdot \mathbf{u}_h\|_{L^2(\Omega_e)} \geq -\frac{1}{2} \left( \frac{1}{\mu} \|p_h\|_{L^2(\Omega_e)}^2 + \mu \|\nabla \mathbf{u}_h\|_{L^2(\Omega_e)}^2 \right), \quad (39)$$

so that

$$\sum_e^{N_e} \left[ \left( \frac{h}{h_e} \right)^2 - 1 \right] \langle p_h, \nabla \cdot \mathbf{u}_h \rangle_{\Omega_e} \geq \frac{1 - C^2}{2} \left( \frac{1}{\mu} \|p_h\|_{L^2(\Omega)}^2 + \mu \|\nabla \mathbf{u}_h\|_{L^2(\Omega)}^2 \right). \quad (40)$$

Furthermore, condition (38) allows us to use an inverse inequality and get

$$\frac{(1 - C^2)}{2} \|p_h\|_{L^2(\Omega)}^2 \geq -\tilde{C} h^2 \|\nabla p_h\|_{L^2(\Omega)}^2. \quad (41)$$

Combining these estimates with Equation (37) gives us

$$A((\mathbf{u}_h, p_h), (\mathbf{u}_h, p_h)) \geq (3 - C^2) \frac{\mu}{2} \|\nabla \mathbf{u}_h\|_{L^2(\Omega)}^2 + (\alpha - \tilde{C}) h^2 \|\nabla p_h\|_{L^2(\Omega)}^2 + \alpha h^2 \langle \nabla p_h \times \mathbf{n}, \mu \nabla \times \mathbf{u}_h \rangle_\Gamma. \quad (42)$$

Thus, guaranteeing that  $A((\mathbf{u}_h, p_h), (\mathbf{u}_h, p_h))$  stays positive would impose a condition on the element sizes, namely,  $C < \sqrt{3}$ , which is obviously too restrictive. We remark, however, that ellipticity is sufficient but not necessary for stability. A stability proof can be done by deriving an appropriate inf-sup condition. This is, at the moment, still an open problem, as well as the formal error analysis of our method. We remark, however, that our numerical experiments with highly nonuniform meshes ( $C > 10$ ) and even adaptive ones for different values of  $\alpha$  do not indicate any apparent signs of stability restrictions. In fact, “pure PPE” formulations such as that by Johnston and Liu<sup>22</sup> also have a “nonvanishing” divergence in the bilinear form and, although a stability proof for  $C^0$  finite elements is also still open in their case,<sup>39</sup> several variations of their method have been used successfully in the past decade in the solution of challenging problems with general meshes,<sup>23,39,42</sup> corner singularities<sup>37,38,40</sup> and wide ranges of Reynolds numbers<sup>24,41</sup>—all providing strong numerical evidence towards good stability properties.

## 4 | DISCRETISATION AND SOLUTION

Standard Lagrangian finite element spaces of equal order for velocity and pressure are considered herein. The corresponding shape functions will be denoted by  $\psi_i$ ,  $i = 1, \dots, N_n$ , with  $N_n$  being the number of nodes in the mesh. Moreover, both simplicial and nonsimplicial elements are considered in the examples. Unless where otherwise stated, first-order pairs are employed.

### 4.1 | The Stokes system

The Stokes solution is obtained by dropping the convective term  $(\rho \nabla \mathbf{u}) \mathbf{u}$ . After discretization, this leads to the linear algebraic system

$$\begin{bmatrix} \mathbf{K} & -\mathbf{B}^\top \\ \alpha^{-1}\tilde{\mathbf{B}} + \mathbf{L} & \mathbf{A} \end{bmatrix} \begin{Bmatrix} \underline{\mathbf{u}} \\ \underline{p} \end{Bmatrix} = \begin{Bmatrix} \underline{\mathbf{b}} \\ \underline{f} \end{Bmatrix}, \quad (43)$$

where  $\mathbf{K}$ ,  $\mathbf{B}$ , and  $\mathbf{b}$  are the usual stiffness matrix, divergence matrix, and forcing vector coming from the standard Galerkin formulation of the Stokes system.<sup>6</sup> Matrix  $\mathbf{A}$  is a standard Laplacian stiffness matrix (without BCs) and matrices  $\mathbf{L}$  and  $\tilde{\mathbf{B}}$  have a block structure:

$$\mathbf{L} = [\mathbf{L}^1 \dots \mathbf{L}^d], \quad \tilde{\mathbf{B}} = [\tilde{\mathbf{B}}^1 \dots \tilde{\mathbf{B}}^d], \quad (44)$$

with

$$L_{ij}^k = \mu \sum_{m=1}^d \int_{\Gamma} (\delta_{mk} - 1) \left( n_m \frac{\partial \psi_i}{\partial x_k} - n_k \frac{\partial \psi_i}{\partial x_m} \right) \frac{\partial \psi_j}{\partial x_m} d\Gamma, \quad (45)$$

$$\tilde{B}_{ij}^k = \mu \sum_{e=1}^{N_e} \frac{1}{h_e^2} \int_{\Omega_e} \psi_i \frac{\partial \psi_j}{\partial x_k} d\Omega, \quad (46)$$

where  $n_k$  is the  $k$ th spatial component of the normal vector  $\mathbf{n}$ , and  $\delta$  is the Kronecker delta. The entries of the forcing term  $\underline{f}$  are given by

$$f_i = \int_{\Omega} \rho \nabla \psi_i \cdot \mathbf{g} d\Omega. \quad (47)$$

## 4.2 | The Navier–Stokes system

When the convection term is kept, an iterative scheme is necessary to solve the resulting nonlinear problem. To obtain such a scheme, standard methods can be readily applied, since the term we add in comparison to classical PSPG is linear. We use the following Picard scheme: after an initial guess  $(\underline{\mathbf{u}}^0, \underline{p}^0)$ , the iterations follow as

$$\begin{bmatrix} \mathbf{K} + \mathbf{C}(\underline{\mathbf{u}}^n) & -\mathbf{B}^\top \\ \alpha^{-1}\tilde{\mathbf{B}} + \mathbf{L} + \mathbf{H}(\underline{\mathbf{u}}^n) & \mathbf{A} \end{bmatrix} \begin{Bmatrix} \underline{\mathbf{u}}^{n+1} \\ \underline{p}^{n+1} \end{Bmatrix} = \begin{Bmatrix} \underline{\mathbf{b}} \\ \underline{f} \end{Bmatrix}, \quad (48)$$

where  $\mathbf{C}$  is a block-diagonal matrix with  $d$  identical blocks  $\mathbf{C}$  given by

$$C_{ij} = \int_{\Omega} \psi_i \nabla \psi_j \cdot \mathbf{u}_h d\Omega, \quad (49)$$

and  $\mathbf{H} = [\mathbf{H}^1 \dots \mathbf{H}^d]$ , with

$$H_{ij}^k = \int_{\Omega} \frac{\partial \psi_i}{\partial x_k} \nabla \psi_j \cdot \mathbf{u}_h d\Omega. \quad (50)$$

After each iteration, Aitken relaxation is applied in order to provide the iterative solver with quadratic convergence<sup>45</sup> (cf. Reference 46 for details).

## 4.3 | Solving the linear system

The linear systems (43) and (48) can be easily solved using direct methods when considering 2D problems, but in three dimensions the resulting memory requirements and computational complexity can quickly become prohibitive. Thus, we present here an iterative technique suitable to handle the problem at hand. It is based on a flexible GMRES method

with right preconditioner  $\mathcal{P}^{-1}$  for the Navier–Stokes system:<sup>47</sup>

$$\mathcal{P}^{-1} := \begin{bmatrix} (\mathbf{K} + \mathbf{C})^{-1} & \mathbf{0} \\ \mathbf{0} & \mathbf{I} \end{bmatrix} \begin{bmatrix} \mathbf{I} & \mathbf{B}^\top \\ \mathbf{0} & \mathbf{I} \end{bmatrix} \begin{bmatrix} \mathbf{I} & \mathbf{0} \\ \mathbf{0} & \mathbf{S}^{-1} \end{bmatrix}, \quad (51)$$

using the Schur complement defined as  $\mathbf{S} := \mathbf{A} + (\alpha^{-1}\tilde{\mathbf{B}} + \mathbf{L} + \mathbf{H})(\mathbf{K} + \mathbf{C})^{-1}\mathbf{B}^\top$ . For the Stokes system, the convective terms in  $\mathcal{P}^{-1}$  and  $\mathbf{S}$  are simply zero. Explicitly computing the Schur complement  $\mathbf{S}$  is considered too costly, so the key factor for achieving robust and fast convergence lies in its efficient approximation. We choose  $\mathbf{S}^{-1} \approx \mu \mathbf{M}_p^{-1}$ , where  $\mathbf{M}_p$  is the mass matrix in the pressure space.<sup>47,48</sup> This choice is suitable for the diffusion-dominated case, which is the focus of this contribution. The actions of the inverses in (51) applied to some iterate can be approximated by single V-cycles of an algebraic multigrid method (e.g., utilizing the BoomerAMG package<sup>49</sup> via deal.II<sup>50</sup>). To further improve scaling, the rows corresponding to the pressure test functions are multiplied by element-averaged factors  $\tau_i$  defined per node as

$$\tau_i := \left( \sum_{e=1}^{N_i} |\Omega_e| \right)^{-1} \sum_{e=1}^{N_i} \frac{\alpha h_e^2}{\mu} |\Omega_e|, \quad (52)$$

where  $|\Omega_e| := \int_{\Omega_e} d\Omega$  and  $N_i$  is the number of elements sharing vertex  $i$ .

## 5 | NUMERICAL EXAMPLES

In this section, we use various benchmark examples to assess the performance of our new method in comparison to classical ones. Triangular, quadrilateral and hexahedral elements are considered. In order to measure approximation errors, we define a normalized  $L^2$  norm

$$\|p - p_h\|_0 := \frac{\|p - p_h\|_{L^2(\Omega)}}{\|p\|_{L^2(\Omega)}},$$

and analogously for  $\mathbf{u}_h$ . The spatial coordinates  $(x_1, x_2, x_3)$  and their corresponding velocity components will be denoted by  $(x, y, z)$  and  $(u, v, w)$ , respectively.

### 5.1 | Stokes flow in the unit circle

We begin with the benchmark case proposed by Weidman.<sup>51</sup> It consists of the Stokes problem in a circular domain with unit radius, centered at the origin, with zero body force and periodic Dirichlet BC  $u_\theta|_\Gamma = \cos n\theta$ , with  $n$  being an integer greater than one,  $u_\theta$  denoting the circumferential velocity and  $\theta := \tan^{-1}(y/x)$ . For  $\mu = 1$  and  $n = 2$ , the analytical solution is

$$\mathbf{u} = \begin{Bmatrix} 2y^3 - y \\ 2x^3 - x \end{Bmatrix}, \quad p = 12xy.$$

For this example we consider a family of seven quasi-uniform triangular meshes, the finest of which is shown in Figure 1 (only an eighth of the mesh is depicted, due to its symmetry). The first goal is to compare our new approach and PSPG, regarding their performance with respect to the stabilization parameter  $\alpha$ . The pressure error for  $\alpha \in [10^{-4}, 10^5]$  using the sixth mesh is shown in Figure 2, and important considerations can be drawn. The expected behavior is observed: the error is large for small values of  $\alpha$ , decreases as  $\alpha$  is increased, reaches a minimum, then starts growing again and eventually settles at a finite value. The two formulations yield similar results for small  $\alpha$ , since the divergence-free constraint dominates over the stabilization term. However, the reasons why each method reaches a limiting performance for  $\alpha \rightarrow \infty$  are distinct. In the PSPG formulation, the error becomes very high because a large  $\alpha$  leads to overrelaxation of incompressibility; in our formulation,  $\alpha \rightarrow \infty$  leads to the PPE completely replacing the divergence-free constraint, which does not violate (discrete) incompressibility but results in suboptimal convergence.<sup>37</sup> Therefore, the error for

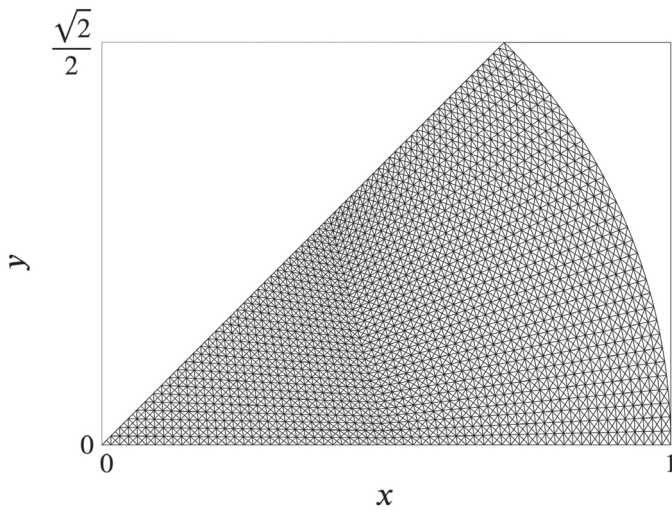


**FIGURE 1** Stokes problem in circular domain: Finest mesh considered in the refinement study (only an eighth is shown)

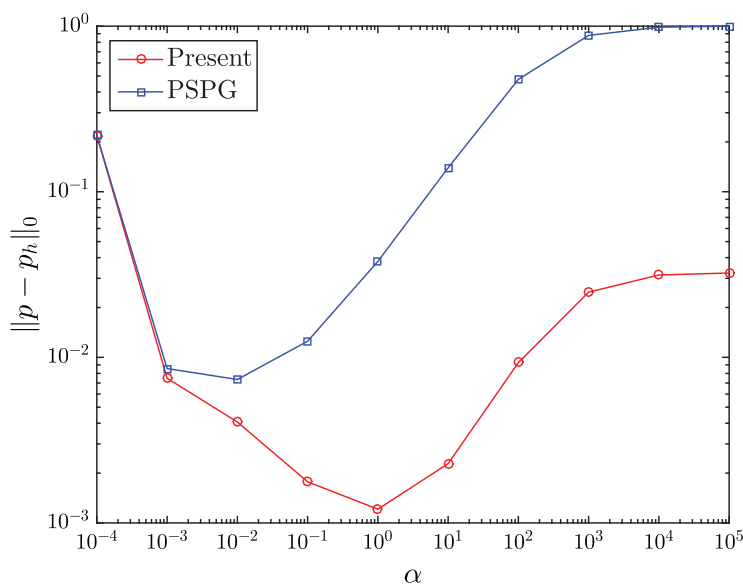


**FIGURE 2** Stokes problem in circular domain: Pressure error with respect to stabilization parameter

large  $\alpha$  is much higher for PSPG than for the present formulation. Moreover, the former's incomplete residual has an important impact on the parameter selection. The numerical solution is very sensitive to the stabilization parameter, with the error growing very fast when  $\alpha$  moves away from its optimal value in either direction. Conversely, in our method the error varies in a smoother way and allows more freedom in the parameter selection. This is a crucial feature for a stabilization technique, since the optimal parameters are often problem- and discretization-dependent. It is also seen that, for this example, the minimum error yielded by our formulation is around one order of magnitude lower than that from PSPG. The velocity errors shown in Figure 3 also reveal the improved accuracy of our formulation.

In order to investigate the issue of spurious pressure boundary layers induced by the incomplete residual, we assess the pressure error in  $L^2(\Gamma)$ , as proposed by Burman and Hansbo.<sup>12</sup> Note that for this example, the PSPG method with linear elements reduces to the original formulation of Brezzi and Pitkäranta,<sup>4</sup> which contains only the term  $\sum_{e=1}^{N_e} \langle \delta_e \nabla q_h, \nabla p_h \rangle_{\Omega_e}$  and therefore induces zero Neumann BCs for the pressure. We also include in the comparison the results attained through the PGP method,<sup>16</sup> which fixes the issue of artificial pressure BCs through an appropriate projection (cf. Section 3.2.3). The plot shown in Figure 4 reveals a similar trend to that attained by edge stabilization methods:<sup>12</sup> we get an additional half an order on the boundary by using the complete residual. This is due to the fact that our formulation is derived from a BVP with consistent pressure BCs.<sup>44</sup> In comparison to edge stabilization methods, ours has the advantage of not requiring operations involving internal edges/faces, which simplifies implementation. It is also seen that our method performs very similarly to the PGP technique, with the advantage of not requiring any projections.

**FIGURE 3** Stokes problem in circular domain: Velocity error with respect to stabilization parameter

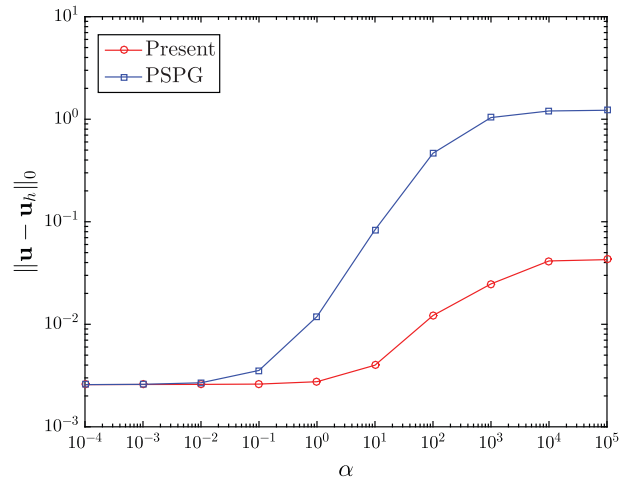
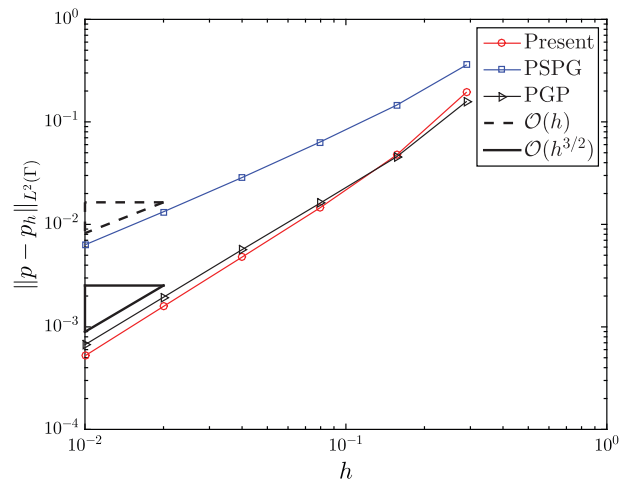


**FIGURE 4** Stokes problem in circular domain: Pressure convergence on the boundary, for  $\alpha = 0.1$



### 5.2 | Kovasznay flow problem

We now consider a nonlinear problem: the Kovasznay flow benchmark.<sup>52</sup> It is one of the only known analytical solutions to the Navier–Stokes problem with  $\mathbf{g} = \mathbf{0}$ , and models the behavior of laminar flow past cylinders. The solution in  $\Omega = \left(-\frac{1}{2}, \frac{1}{2}\right)^2$  is

$$\mathbf{u} = \begin{Bmatrix} 1 - e^{kx} \cos 2\pi y \\ \frac{k}{2\pi} e^{kx} \sin 2\pi y \end{Bmatrix}, \quad p = \frac{e^k - e^{2kx}}{2},$$

where  $\text{Re}$  is the Reynolds number and  $k = \frac{\text{Re}}{2} - \sqrt{\left(\frac{\text{Re}}{2}\right)^2 + (2\pi)^2}$ . We solve the corresponding Dirichlet problem using linear triangular elements. The coarsest mesh is shown in Figure 5, and then seven levels of uniform refinement are considered. The pressure and velocity errors for  $\text{Re} = 100$  and  $\alpha = 1$  are shown in Figure 6. We observe that, although both PSPG and our formulation converge with similar rates, the former takes longer to reach the asymptotic behavior, which leads to larger errors. The reason for this “delayed” convergence is the fact that the artificial pressure BCs induced by the PSPG formulation only become negligible as the mesh size goes to zero.<sup>6</sup> Another important finding from the convergence plots is the remarkable performance gain of our approach with respect to the pure PPE formulation,<sup>22</sup> through the addition of a simple term to penalize large velocity divergences.

To further illustrate how the incomplete residual can impact the quality of the approximation, we show in Figure 7 the pressure isolines for the Kovasznay problem with  $\text{Re} = 40$ ,  $\alpha = 100$  and the third finest mesh considered in the

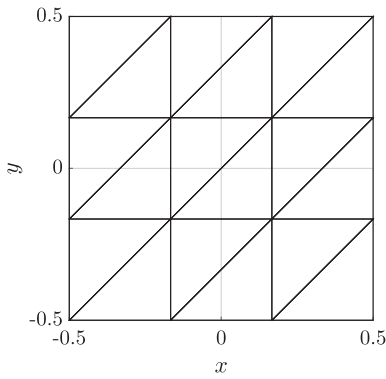


**FIGURE 5** Kovaszny benchmark: Coarsest mesh used in the refinement study

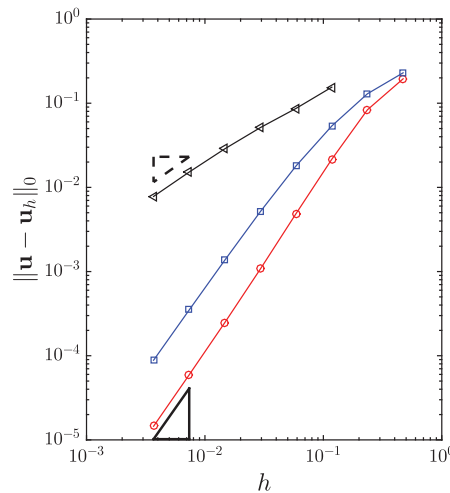
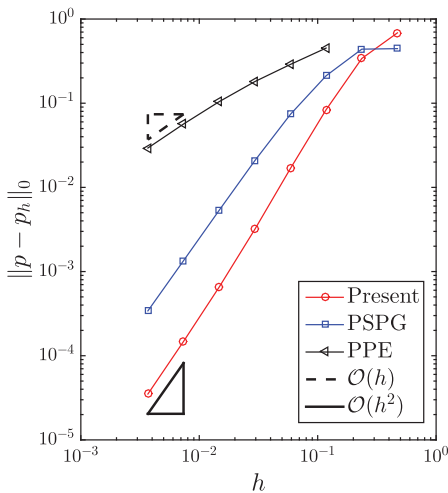


**FIGURE 6** Kovaszny benchmark: Uniform refinement study

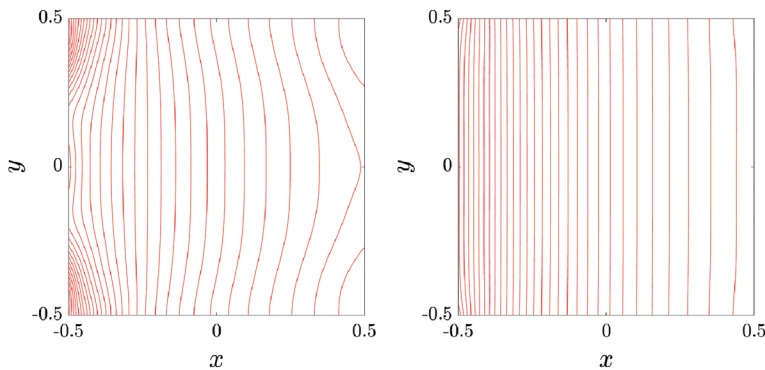


**FIGURE 7** Kovaszny benchmark: Pressure isolines for PSPG (left) and present formulation (right)

convergence study. This is a particularly good example for illustrating the issue of spurious pressure boundary layers, since the exact solution has perfectly vertical isolines. Note that the stabilization parameter is deliberately chosen outside of the optimal interval for both formulations, so as to critically test their performance. We see that PSPG yields completely distorted lines all over the domain, whereas in our approach there is only a mild distortion close to the corners.

It is also of interest to investigate how our method performs in combination with equal-order spaces of higher polynomial degree, since they are able to approximate the Laplacian in the standard PSPG residual. We investigate that by assessing the effect of the stabilization parameter  $\alpha$  for elements of type  $Q_k Q_k$ , that is, equal-order quadrilateral elements with polynomial degree up to  $k$  in each direction. We consider a  $64 \times 64$  uniform grid,  $\text{Re} = 100$  and  $k = 1, 2, 3, 4$ . The results depicted in Figure 8 reveal once again an increase in accuracy for a wider range of  $\alpha$ . This is due to the fact that, even though the PSPG residual is complete for  $k > 1$ , large  $\alpha$  leads to an overrelaxation of the incompressibility constraint, which does not happen in our PPE-based formulation. Especially for  $k = 4$ , the approximation attained by our method has

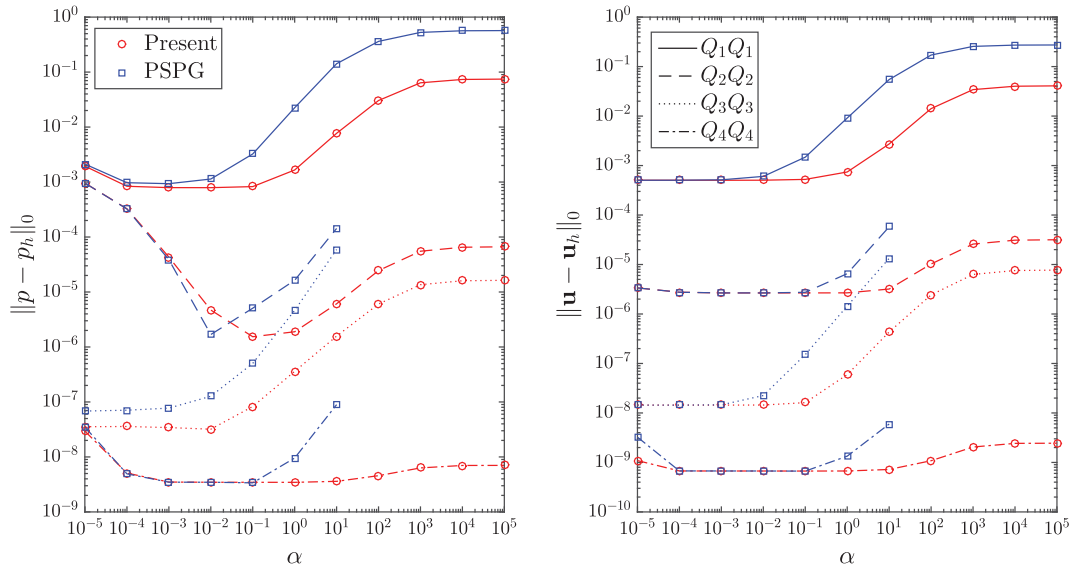


**FIGURE 8** Kovaszny benchmark: Error with respect to stabilization parameter for higher-order elements

**FIGURE 9** Kovaszny benchmark in anisotropic meshes: Coarsest mesh used in the refinement study

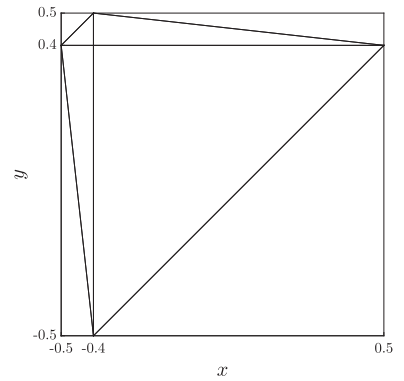
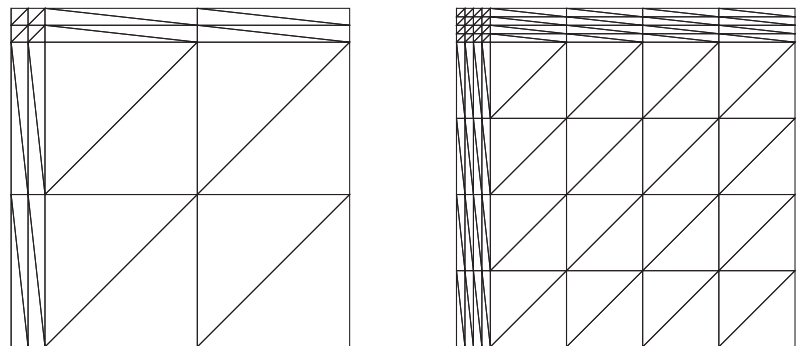


**FIGURE 10** Kovaszny benchmark in anisotropic meshes: First and second refinement levels



proven considerably less sensitive to the choice of stabilization parameter. Note that for  $\alpha > 10$  the solution of the PSPG method (considering zero initial guess for the iterative scheme) diverged.

In order to put our method to a more challenging test, we use now anisotropic, highly nonuniform meshes. The coarsest mesh is shown in Figure 9, where we can see that the element size varies by a factor of up to 9 between adjacent elements—a rather extreme setting. The second and third meshes are shown in Figure 10, and the refinement goes on uniformly. The pressure and velocity errors for  $\alpha = 10$  are depicted in Figure 11, where we can verify good stability and convergence behavior, as in previous examples. Results for graded 3D meshes are also in agreement with these findings, as we show next.

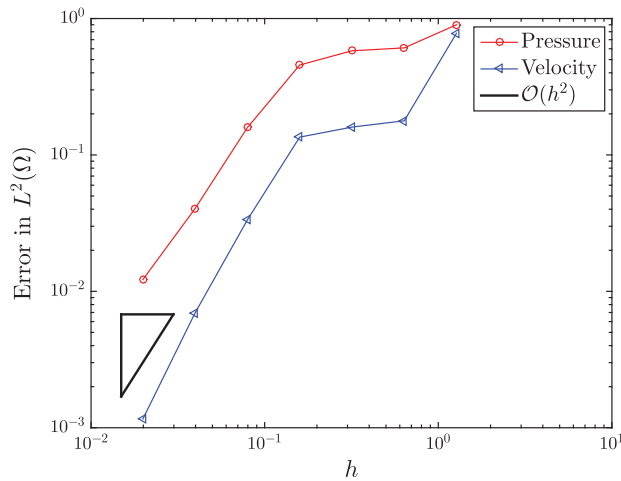


**FIGURE 11** Kovaszny benchmark: Refinement study with anisotropic meshes

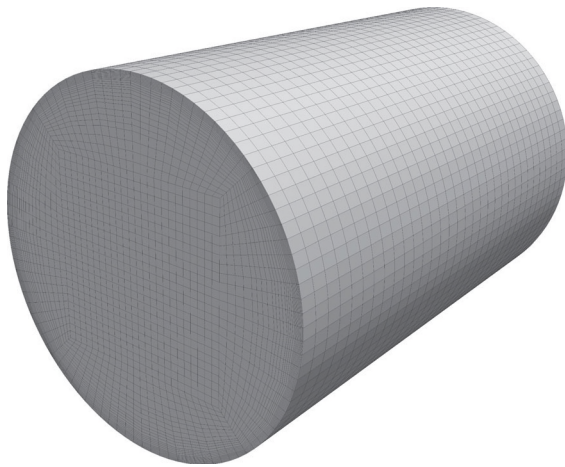


**FIGURE 12** Poiseuille flow: Graded mesh used for the first test case

### 5.3 | Poiseuille flow in three dimensions

We now consider a 3D example on graded hexahedral meshes. The domain is a cylinder defined as

$$\Omega = \{(x, y, z) \in \mathbb{R}^3 : x^2 + y^2 < R^2, 0 < z < L\}.$$

The corresponding Poiseuille flow solution is

$$\mathbf{u} = \left\{ 0, 0, \frac{2Q}{\pi R^2} \left( 1 - \frac{x^2 + y^2}{R^2} \right) \right\}^T, \quad p = \frac{8\mu QL}{\pi R^4} \left( 1 - \frac{z}{L} \right),$$

in which  $Q$  is a given volumetric flow rate and  $R$  and  $L$  are the pipe's radius and length, respectively. There are no body forces. As BCs for the numerical solution, we use the analytical velocity profile on the inlet  $z=0$ , no-slip on the wall ( $x^2 + y^2 = R^2$ ) and zero natural BC ( $\mathbf{t}_N = \mathbf{0}$ ) on the outlet  $z=L$ . We begin once again by comparing the methods regarding the effect of the stabilization parameter  $\alpha$ . For this, we consider a test case with  $\frac{L}{R} = 3$ ,  $\text{Re} = 150$  and a graded mesh with 92160 elements and 96657 nodes (see Figure 12). For this example, too, our method clearly outperforms PSPG in accuracy and sensitivity with respect to  $\alpha$ , as revealed by the error plot in Figure 13—even though the velocity Laplacian is not zero everywhere for non-Cartesian hexahedral meshes, as the present one.

Next, a convergence study is performed for the present method. The four graded meshes considered are depicted in Figure 14 (frontal view). The refinement in the  $z$  direction is uniform, starting with an element length of  $L/3$ . We consider a normalized problem with  $\frac{2R}{L} = \frac{\rho Q}{\mu R} = 1$ . As for the 2D examples, we use a direct solver here. Table 1 shows the errors for the four meshes. Once again, the estimated orders of convergence (eoc) are quadratic. It is important to draw some



**FIGURE 13** Poiseuille flow: Error with respect to stabilization parameter

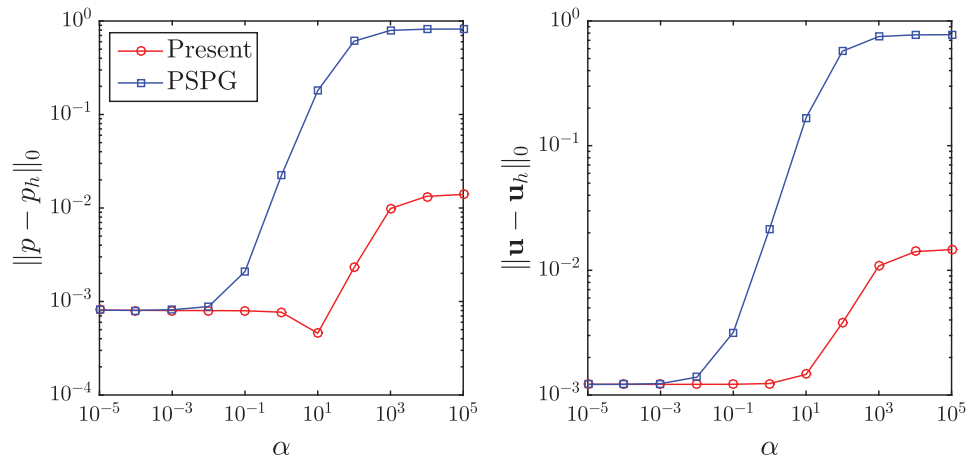


**FIGURE 14** Frontal view of the graded meshes used for the Poiseuille flow problem

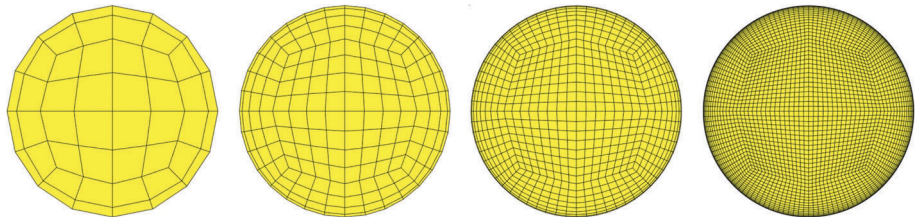


**TABLE 1** Poiseuille flow: Convergence study for graded meshes

Mesh	$\ \mathbf{u} - \mathbf{u}_h\ _0$	eoc	$\ p - p_h\ _0$	eoc
1	$7.2 \times 10^{-2}$	–	$3.5 \times 10^{-2}$	–
2	$1.3 \times 10^{-2}$	2.4	$6.0 \times 10^{-3}$	2.5
3	$3.3 \times 10^{-3}$	2.0	$1.5 \times 10^{-3}$	2.0
4	$8.3 \times 10^{-4}$	2.0	$3.6 \times 10^{-4}$	2.0

remarks regarding the convergence rates. From the approximation standpoint, the polynomial degree for  $p_h$  should be one less than for  $\mathbf{u}_h$  to guarantee quadratic pressure convergence, since we are looking for  $p \in L^2(\Omega)$  but  $\mathbf{u} \in [H^1(\Omega)]^d$ . When using equal orders, all that can be guaranteed for the pressure is at least linear convergence in  $L^2(\Omega)$ .<sup>5,8</sup> As a matter of fact, the order is known in practice to range between 1 and 2, depending on the flow regime.<sup>6</sup> Therefore, the quadratic convergence experienced here for the pressure should be seen as an “initial” higher-order convergence<sup>53</sup> and cannot be expected to hold indefinitely and for all problems. This applies of course not only to our formulation, but to equal-order methods in general.<sup>4,5,8,13,16,25</sup>

### 5.4 | Lid-driven cavity flow

As a final example, we consider the classical lid-driven cavity benchmark with  $Re = 5000$ . It consists of flow confined in the unit square  $\Omega = (0, 1)^2$ , driven by discontinuous Dirichlet BCs:  $\mathbf{u} = \{1, 0\}^T$  at  $y = 1$ , and  $\mathbf{u} = \mathbf{0}$  on the remaining walls. This is a more challenging problem due to the higher Reynolds number and the pressure singularity induced by the discontinuous BCs. To solve the BC ambiguity at the upper corner nodes, we apply the regularization proposed by de Frutos et al.<sup>54</sup> A uniform mesh with  $128 \times 128$  square elements has been considered, with a constant parameter  $\gamma = 0.3/h$  for the stabilization. Figure 15 shows the comparison between our results and those attained by Erturk et al.,<sup>55</sup> in terms of velocity components. Excellent agreement is observed between the solutions. In Figure 16, we see that the pressure approximation presents no apparent spurious oscillations, in spite of its clear nonsmooth character.

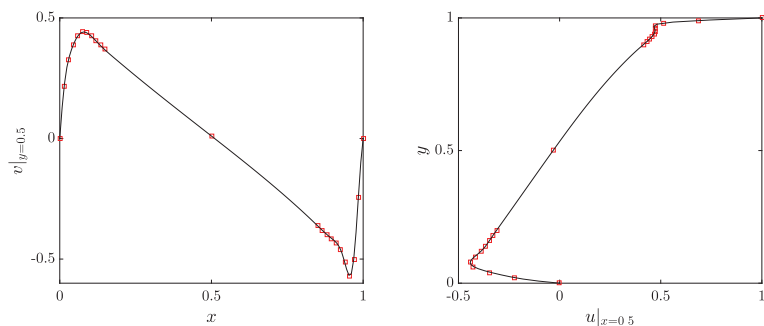


**FIGURE 15** Lid-driven cavity flow: Comparison between present results (lines) and those by Erturk et al.<sup>55</sup> (markers)

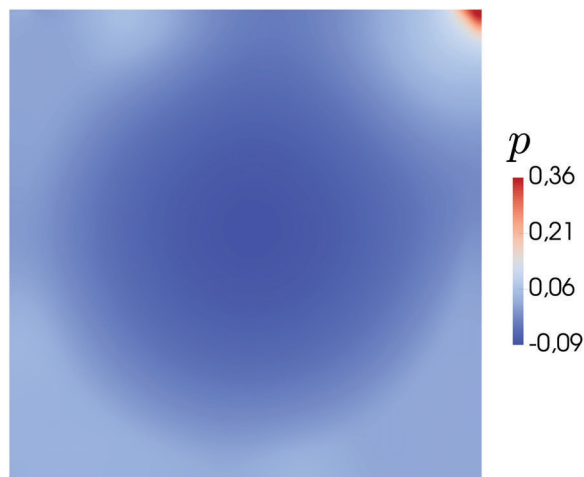


**FIGURE 16** Lid-driven cavity flow: Pressure distribution

## 6 | CONCLUDING REMARKS

This work has presented a global pressure-stabilized formulation for incompressible flows allowing equal-order velocity-pressure pairs. The method can be derived by replacing the standard Navier–Stokes equations by an equivalent system containing a weighted average of the continuity equation and the PPE. Using such an equivalent BVP and appropriate vector calculus identities, we rewrite the second-order viscous term as a first-order boundary term, thereby preserving the viscous part of the residual even for lowest-order elements. To the best of our knowledge, this is the first stabilization technique which allows a complete evaluation of the residual for first-order elements without requiring the definition of auxiliary variables and projections, or unconventional data structures such as macroelements, patches and internal face loops. Furthermore, our method does not rely on a relaxation of incompressibility, as opposed to most standard pressure stabilization methods. Various numerical examples have been tackled to provide an appropriate comparison between our formulation and existing ones, revealing a clear gain in accuracy and flexibility with respect to the stabilization parameter, for lowest- and higher-order elements. In particular, our method improves the approximation around the boundaries by alleviating spurious pressure boundary layers. We hope that this new tool can offer the computational fluid dynamics community a practical, efficient alternative to some existing techniques such as PSPG and edge stabilization methods. Future and ongoing developments include a generalization to fluids with variable viscosity,<sup>56</sup> as well as a systematic numerical analysis to provide theoretical stability estimates. Also ongoing is the development of robust solvers for the stabilized system in general flow regimes, including suitable preconditioners and adaptive stepping for time-dependent problems.

## ACKNOWLEDGMENTS


The authors acknowledge Graz University of Technology for the financial support of the Lead-project: Mechanics, Modeling and Simulation of Aortic Dissection. We also wish to thank the reviewers for their invaluable advice and thorough examination of our work.

## DATA AVAILABILITY STATEMENT

Data sharing not applicable to this article as no datasets were generated or analyzed during the current study.

## ORCID

Douglas R. Q. Pacheco  <https://orcid.org/0000-0002-3494-7118>

Thomas-Peter Fries  <https://orcid.org/0000-0003-1210-1557>

## REFERENCES

1. Donea J, Huerta A. *Finite Element Methods for Flow Problems*. New York, NY: John Wiley & Sons; 2003.
2. Boffi D, Brezzi F, Fortin M. *Mixed Finite Element Methods and Applications*. New York, NY: Springer; 2013.
3. Hood P, Taylor C. Navier-Stokes equations using mixed interpolation. In: Oden JT, Zienkiewicz OC, Gallagher RH, Taylor C, eds. *Finite Element Methods in Flow Problems*. Huntsville, Alabama: UAH Press; 1974:57-66.
4. Brezzi F, Pitkäranta J. On the stabilization of finite element approximations of the Stokes equations. In: Hackbusch W, ed. *Efficient Solutions of Elliptic Systems*. Notes on Numerical Fluid Mechanics. Wiesbaden, Germany: Vieweg+ Teubner Verlag; 1984:11-19.
5. Hughes TJR, Franca LP, Balestra M. A new finite element formulation for computational fluid dynamics: V. circumventing the Babuška-Brezzi condition: a stable Petrov-Galerkin formulation of the Stokes problem accommodating equal-order interpolations. *Comput Methods Appl Mech Eng*. 1986;59(1):85-99.
6. John V. *Finite Element Methods for Incompressible Flow Problems*. New York, NY: Springer; 2016.
7. Hughes TJR, Franca LP. A new finite element formulation for computational fluid dynamics: VII. the Stokes problem with various well-posed boundary conditions: symmetric formulations that converge for all velocity/pressure spaces. *Comput Methods Appl Mech Eng*. 1987;65(1):85-96.
8. Brezzi F, Douglas J Jr. Stabilized mixed methods for the Stokes problem. *Numer Math*. 1988;53(1-2):225-235.
9. Douglas J Jr, Wang J. An absolutely stabilized finite element method for the Stokes problem. *Math Comput*. 1989;52(186):495.
10. Droux J-J, Hughes TJR. A boundary integral modification of the Galerkin least squares formulation for the Stokes problem. *Comput Methods Appl Mech Eng*. 1994;113(1-2):173-182.
11. Jansen KE, Collis SS, Whiting C, Shaki F. A better consistency for low-order stabilized finite element methods. *Comput Methods Appl Mech Eng*. 1999;174(1-2):153-170.
12. Burman E, Hansbo P. Edge stabilization for the generalized Stokes problem: a continuous interior penalty method. *Comput Methods Appl Mech Eng*. 2006;195(19-22):2393-2410.
13. Bochev P, Gunzburger M. An absolutely stable pressure-poisson stabilized finite element method for the Stokes equations. *SIAM J Numer Anal*. 2004;42(3):1189-1207.
14. Becker R, Braack M. A finite element pressure gradient stabilization for the Stokes equations based on local projections. *Calcolo*. 2001;38(4):173-199.
15. Braack M, Lube G. Finite elements with local projection stabilization for incompressible flow problems. *J Comput Math*. 2009;27:116-147.
16. Codina R, Blasco J. A finite element formulation for the Stokes problem allowing equal velocity-pressure interpolation. *Comput Methods Appl Mech Eng*. 1997;143(3-4):373-391.
17. Codina R, Blasco J, Buscaglia GC, Huerta A. Implementation of a stabilized finite element formulation for the incompressible Navier-Stokes equations based on a pressure gradient projection. *Int J Numer Methods Fluids*. 2001;37(4):419-444.
18. Hughes TJR, Liu WK, Brooks A. Finite element analysis of incompressible viscous flows by the penalty function formulation. *J Comput Phys*. 1979;30(1):1-60.
19. Nithiarasu P. A fully explicit characteristic based split(CBS) scheme for viscoelastic flow calculations. *Int J Numer Methods Eng*. 2004;60(5):949-978.
20. Nithiarasu P, Liu C-B. An artificial compressibility based characteristic based split (CBS) scheme for steady and unsteady turbulent incompressible flows. *Comput Methods Appl Mech Eng*. 2006;195(23-24):2961-2982.
21. Franca LP, Russo A. Approximation of the Stokes problem by residual-free macro bubbles. East-West. *J Numer Math*. 1996;4:265-278.
22. Johnston H, Liu J-G. Accurate, stable and efficient Navier-Stokes solvers based on explicit treatment of the pressure term. *J Comput Phys*. 2004;199(1):221-259.
23. Liu J. Open and traction boundary conditions for the incompressible Navier-Stokes equations. *J Comput Phys*. 2009;228(19):7250-7267.
24. Shirokoff D, Rosales RR. An efficient method for the incompressible Navier-Stokes equations on irregular domains with no-slip boundary conditions, high order up to the boundary. *J Comput Phys*. 2011;230(23):8619-8646.
25. Dohrmann CR, Bochev PB. A stabilized finite element method for the Stokes problem based on polynomial pressure projections. *Int J Numer Methods Fluids*. 2004;46(2):183-201.
26. Franca LP, Frey SL. Stabilized finite element methods: II. the incompressible Navier-Stokes equations. *Comput Methods Appl Mech Eng*. 1992;99(2-3):209-233.
27. Franca LP, Hughes TJR. Two classes of mixed finite element methods. *Comput Methods Appl Mech Eng*. 1988;69(1):89-129.
28. Olshanskii M, Lube G, Heister T, Löwe J. Grad-div stabilization and subgrid pressure models for the incompressible Navier-Stokes equations. *Comput Methods Appl Mech Eng*. 2009;198(49-52):3975-3988.
29. Hartmann R. Higher-order and adaptive discontinuous Galerkin methods with shock-capturing applied to transonic turbulent delta wing flow. *Int J Numer Methods Fluids*. 2013;72(8):883-894.
30. Franca LP, Hughes TJR, Stenberg R. Stabilized finite element methods. In: Gunzburger MD, Nicolaides RA, eds. *Incompressible Computational Fluid Dynamics: Trends and Advances*. Cambridge, MA: Cambridge University Press; 1993:87-107.

31. John V, Knobloch P, Wilbrandt U. Finite element pressure stabilizations for incompressible flow problems. In: Bodnár T, Galdi G, Nečasová Š, eds. *Fluids Under Pressure. Advances in Mathematical Fluid Mechanics*. Basel, Switzerland: Birkhäuser; 2020:483-573.
32. Fries T-P, Matthies HG. A stabilized and coupled meshfree/meshbased method for the incompressible Navier–Stokes equations Part II: coupling. *Comput Methods Appl Mech Eng*. 2006;195(44-47):6191-6204.
33. Gresho PM. Some current CFD issues relevant to the incompressible Navier-Stokes equations. *Comput Methods Appl Mech Eng*. 1991;87(2-3):201-252.
34. Heywood JG, Rannacher R, Turek S. Artificial boundaries and flux and pressure conditions for the incompressible Navier-Stokes equations. *Int J Numer Methods Fluids*. 1996;22(5):325-352.
35. Heywood JG, Rannacher R. Finite element approximation of the nonstationary Navier–Stokes problem. I. regularity of solutions and second-order error estimates for spatial discretization. *SIAM J Numer Anal*. 1982;19(2):275-311.
36. Sani RL, Shen J, Pironneau O, Gresho PM. Pressure boundary condition for the time-dependent incompressible Navier–Stokes equations. *Int J Numer Methods Fluids*. 2006;50(6):673-682.
37. Liu J-G, Liu J, Pego RL. Stable and accurate pressure approximation for unsteady incompressible viscous flow. *J Comput Phys*. 2010;229(9):3428-3453.
38. Liu J-G, Liu J, Pego RL. Error estimates for finite-element Navier-Stokes solvers without standard Inf-Sup conditions. *Chin Ann Math Ser B*. 2009;30(6):743-768.
39. Jia J, Liu J. Stable and spectrally accurate schemes for the Navier–Stokes equations. *SIAM J Sci Comput*. 2011;33(5):2421-2439.
40. Sheng Z, Thiriet M, Hecht F. A high-order scheme for the incompressible Navier-Stokes equations with open boundary condition. *Int J Numer Methods Fluids*. 2013;73(1):58-73.
41. Johnston H, Wang C, Liu J-G. A local pressure boundary condition spectral collocation scheme for the three-dimensional Navier–Stokes equations. *J Sci Comput*. 2014;60(3):612-626.
42. Li L. A split-step finite-element method for incompressible Navier-Stokes equations with high-order accuracy up-to the boundary. *J Comput Phys*. 2020;408:109274.
43. Schöberl J. Numerical Methods for Maxwell Equations. Lecture Note; 2009.
44. Gresho PM, Sani RL. On pressure boundary conditions for the incompressible Navier-Stokes equations. *Int J Numer Methods Fluids*. 1987;7(10):1111-1145.
45. Verzhbitski VM, Yumanova IF. On the quadratic convergence of the Aitken  $\Delta^2$  process. *Comput Math Math Phys*. 2011;51(10):1659-1663.
46. Küttler U, Wall WA. Fixed-point fluid-structure interaction solvers with dynamic relaxation. *Comput Mech*. 2008;43(1):61-72.
47. Turek S. *Efficient Solvers for Incompressible Flow Problems: An Algorithmic and Computational Approach*. Berlin, Germany: Springer; 1999.
48. Cahouet J, Chabard J. ?P. Some fast 3D finite element solvers for the generalized Stokes problem. *Int J Numer Methods Fluids*. 1988;8(8):869-895.
49. Henson VE, Yang UM. BoomerAMG: a parallel algebraic multigrid solver and preconditioner. *Appl Numer Math*. 2000;41:155-177.
50. Alzetta G, Arndt D, Bangerth W, et al. The deal.II library, version 9.0. *J Numer Math*. 2018;26(4):173-183.
51. Weidman PD. Flows induced by the surface motions of a cylindrical sheet. *J Eng Math*. 2010;68(3-4):355-372.
52. Kovasznay LIG. Laminar flow behind a two-dimensional grid. *Math Proc Cambridge Philos Soc*. 1948;44(1):58-62.
53. Steinbach O. A note on initial higher-order convergence results for boundary element methods with approximated boundary conditions. *Numer Methods Part Differ Equat*. 2000;16(6):581-588.
54. de Frutos J, John V, Novo J. Projection methods for incompressible flow problems with WENO finite difference schemes. *J Comput Phys*. 2016;309:368-386.
55. Erturk E, Corke TC, Gökçöl C. Numerical solutions of 2-D steady incompressible driven cavity flow at high Reynolds numbers. *Int J Numer Methods Fluids*. 2005;48(7):747-774.
56. Pacheco DRQ, Steinbach O. A continuous finite element framework for the pressure Poisson equation allowing non-Newtonian and compressible flow behavior. *Int J Numer Methods Fluids*. 2020. <https://doi.org/10.1002/flid.4936>.

**How to cite this article:** Pacheco DRQ, Schussnig R, Steinbach O, Fries T-P. A global residual-based stabilization for equal-order finite element approximations of incompressible flows. *Int J Numer Methods Eng*. 2021;122:2075–2094. <https://doi.org/10.1002/nme.6615>